ELSEVIER

Gaucher Disease Patient With Myoclonus Epilepsy and a Novel Mutation

Asako Tajima, MD*,
Toya Ohashi, MD, PhD*†,
Shin-ichiro Hamano, MD, PhD*‡,
Norimichi Higurashi, MD*‡, and
Hiroyuki Ida, MD, PhD*,

The *N188S* mutation in Gaucher disease is associated with myoclonus epilepsy. We performed genetic analysis on a patient with progressive myoclonus epilepsy, who had received antiepileptic drugs for over 10 years. We detected *N188S/G199D* on the gene encoding glucocerebrosidase. Mutant proteins carrying each mutation were expressed in COS-1 cells (a commonly used cell line which derives from kidney cells of the African green monkey). Measurements of enzymatic activity and Western blotting analysis were performed. When residual activities were measured, glucocerebrosidase with the *N188S* mutation exhibited 50% activity of the wild type, and with *G199D*, 7.4%. Neither mutation influenced the stability of the enzyme protein. These data suggested a diagnosis of Gaucher disease for this patient, and indicated that *G199D* is a novel mutation.

Tajima A, Ohashi T, Hamano S, Higurashi N, Ida H. Gaucher disease patient with myoclonus epilepsy and a novel mutation. Pediatr Neurol 2010;42:65-68.

Introduction

Gaucher disease is the most prevalent lysosomal storage disease, and is caused by more than 200 mutations that produce abnormal glucocerebrosidase. Gaucher disease exhibits a wide range of phenotypes, most of which cannot be explained by a correlation with a specific genotype. Types 2 and 3 of Gaucher disease comprise the neuronopathic forms of the disease, and present various central nervous system manifestations. One of these manifestations is myoclonus epilepsy, and although it is rare, more Gaucher patients presenting with myoclonus epilepsy are found.

The myoclonus epilepsy evident in Gaucher disease and its relationship to the *N188S* mutation were discussed previously. The first report of *N188S* from Kim et al. suggested that this mutation might be a protective gene for neuronopathic forms of Gaucher disease such as the *N370S* mutation [1]. However, considering the results of other studies, *N188S* carriers retain the possibility to develop myoclonic seizures [2-4], although the exact correlation remains unknown.

We report on a 16-year-old girl with intractable epileptic seizures, including myoclonus, who was finally diagnosed as manifesting Gaucher disease. We detected *N188S/G199D* by sequencing and restriction fragment length polymorphism analysis. *G199D* is a novel mutation, and this study describes the genetic and functional analyses of these mutations.

Case Report

Patient

A 16-year-old girl with epileptic seizures and a diagnosis of Gaucher disease was referred to our institution for genetic analysis. She first presented with generalized seizures at age 1 year. An electroencephalogram and computed tomography of the brain produced normal results, and she was diagnosed as manifesting epilepsy. She did not exhibit other neurologic signs until age 5 years, when she presented with absence epilepsy. Developmental delay had become apparent by the time she entered primary school. Valproic acid was not effective for treating the absence seizures, and other anticonvulsants were used. Her seizures improved with valproic acid, ethosuximide, and clonazepam for a few years. At age 11 years, she began to manifest generalized tonic-clonic seizures that occurred more and more frequently. Action tremors had also appeared, followed by motor ataxia, myoclonus, and supranuclear gaze palsy, which together suggested progressive myoclonus epilepsy. Vertical supranuclear gaze palsy was initially evident. Horizontal ocular movement also became restricted at age 18 years. Myoclonus was easily induced by mere contact, which made it very difficult for her to walk, and the antiepileptic drugs no longer controlled her seizures. Phenobarbital was added, but the seizures continued. However, after the administration of piracetam, she could walk again. Upon her admission to the hospital at age 16 years for further examination and to establish a diagnosis, she could sit alone and was able to walk, using a wide-based gait, with support. On admission, hepatosplenomegaly and

From the *Department of Pediatrics, and †Department of Gene Therapy, Institute of DNA Medicine, Jikei University School of Medicine, Tokyo, Japan; and ‡Division of Neurology, Saitama Children's Medical Center, Saitama, Japan.

Communications should be addressed to:
Dr. Tajima; Department of Pediatrics, Jikei University School of Medicine; 3-25-8 Nishi-shinbashi, Minato-ku; Tokyo 105-8461, Japan.
E-mail: atajima@jikei.ac.jp
Received February 9, 2009; accepted August 12, 2009.

doi:10.1016/j.pediatrneurol.2009.08.007 • 0887-8994/10/$—see front matter

anemia were not evident. However, her platelet counts were low, at $9.9 \times 10^4/\mu L$. The level of angiotensin-converting enzyme was 20.0 U/L (normal, 7.0-25.0 U/L), and her level of acid phosphatase was 10.6 U/L (normal, 5.9-14.0 U/L). No abnormal signal was evident according to magnetic resonance imaging of the brain. An electroencephalogram revealed mainly α-waves with diffuse polyspike bursts. The differential diagnosis for progressive cerebellar ataxia and myoclonus includes lysosomal disease. Therefore, pathologic observations of the bone marrow were essential. Bone marrow aspiration using light microscopy revealed cells with a "sandpaper" appearance that resembled Gaucher cells (Fig 1). Because these observations suggested a lysosomal disease, we acquired informed consent from the parents, and analyzed the activities of various enzymes related to lysosome. Glucocerebrosidase activity was reduced in fibroblasts, to about 26% of normal control levels. However, this residual activity was relatively high compared with that of a known patient with Gaucher disease. Usually, patients with Gaucher disease demonstrate less than 10% enzyme activity (Table 1). Gaucher disease was suspected, and a genetic analysis was performed to confirm the diagnosis, after receiving informed consent from the parents. Serum glucosylceramide and chitotriosidase measurements were not performed because they were not commercially available in Japan.

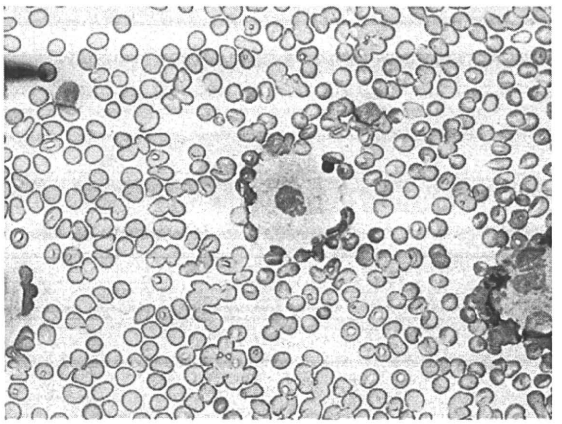

Figure 1. Light microscopy of a bone marrow aspiration (original magnification ×100). A cell with a "sandpaper" appearance was evident.

Genetic Analysis

We extracted DNA from white blood cells of the patient. Initially, eight common mutations in Gaucher disease (*N370S*, *L444P*, *F213I*, *84GG*, *IVS2+1*, *D409H*, *R463C*, and *RecNciI*) were tested as described by Ida et al. [5-7]. However, because none of these mutations were identified, all exonic regions were amplified by polymerase chain reaction using Takara PCR Thermal Cycler (Takara Bio Inc., Otsu, Shiga, Japan), followed by single-strand conformation polymorphism analysis. Single-strand conformation polymorphism analysis revealed a shifted band in exon 6, and direct sequencing was performed using ABI Prism Model 3700 (Applied Biosystems, Foster City, CA). We identified *N188S* and *G199D* mutations in the same exon. Restriction fragment length polymorphism analysis was performed, and the polymerase chain reaction fragment was digested with *Tsp*RI or *Mbo*I to confirm the genotype. We also analyzed the parents' glucocerebrosidase gene, and learned that the parents carried both mutations heteroallelically.

Expression Analysis

To demonstrate that the two detected mutations caused reductions in glucocerebrosidase activity, mutant proteins carrying each of the mutations were produced. Each mutation was generated into glucocerebrosidase complementary DNA by using a QuikChange II Site-Directed Mutagenesis Kit (Stratagene, La Jolla, CA). The primers for exon 6 consisted of 5′-ATACCCCTGATTCACCGAGC-3′ (sense) and 5′-ACCCGGTCTAT GAAACACTT-3′ (antisense). After inserting the mutant complementary DNAs into pCDN6 plasmid, plasmids were transfected into COS-1, using Lipofectamine 2000 (Invitrogen, Carlsbad, CA).

After 48 hours, COS-1 cells were harvested, and glucocerebrosidase activities in the cells were measured using 4-methylumbelliferyl-β-glucopyranoside as a substrate, as described elsewhere [6]. The reaction was halted by adding 0.17 M glycine carbonate buffer (pH 10.4), and enzyme activity was measured by a spectrofluorophotometer, using RF-5300PC (Shimadzu, Tokyo, Japan). Residual glucocerebrosidase activities are described in Fig 2. Glucocerebrosidase activity was reduced in both mutants, and especially in the protein with *G199D*. The *N188S* mutant glucocerebrosidase demonstrated about 50% activity of the normal control, consistent with a previous report [8]. On the other hand, the *G199D*-bearing allele produced an enzyme with no significant activity. These results proved that *G199D* is a novel mutation that causes Gaucher disease, and the diagnosis of our patient was confirmed.

To determine whether glucocerebrosidase carrying the *N188S* or *G199D* mutation influenced protein stability, Western blotting analysis was performed. Proteins were subjected to sodium dodecyl sulfate polyacrylamide gel electrophoresis (10% polyacrylamide), and electrophoretically transferred onto nitrocellulose membranes. The membrane was blocked with 3% gelatin in Tris-buffered saline for 30 minutes, and washed with Tris-buffered saline containing 0.05% Tween-20. The membrane was then incubated with a polyclonal rabbit anti-glucocerebrosidase antibody for 1 hour at room temperature, and washed with Tris-buffered saline containing 0.05% Tween-20 (the antibody was produced by Toya Ohashi, MD, PhD, Department of Gene Therapy, Institute of DNA Medicine, Jikei University School of Medicine, Tokyo, Japan). After incubation with a goat anti-rabbit immunoglobulin G(H + L) alkaliphosphatase antibody (BioRad, Hercules, CA) for 1 hour, the membrane was washed with Tris-buffered saline containing 0.05% Tween-20 and Tris-buffered saline. The immunoreactive bands were detected using an AP Conjugate Substrate Kit (BioRad). The amounts of expressed proteins did not differ significantly (data not shown).

Discussion

In this study, we detected *N188S/G199D* in a glucocerebrosidase gene from a patient with myoclonus epilepsy. *G199D* was an unknown missense mutation, and therefore, to clarify its function and confirm that this mutation profoundly influences enzymatic activity, we performed Western blotting analysis and enzymatic analysis. Both experiments proved that *G199D* reduces glucocerebrosidase activity (7% of the wild type in this study) and leads to the onset of Gaucher disease. Moreover, the very low activity suggests that *G199D* is a null mutation. Although more cases are needed for confirmation, *G199D* is one of the mutations to be considered when evaluating a patient with Gaucher disease. On the other hand, *N188S* was previously demonstrated to exert a mild effect on glucocerebrosidase activity. Moreover, when *N188S* was expressed in COS-1 cells, enzymatic activity was only decreased to 50% of the wild type. Because of this relatively highly restored activity, we wondered whether *N188S* is really responsible for Gaucher disease. However, as we have mentioned, some patients with Gaucher disease and myoclonus epilepsy possess this mutation. Furthermore, we found cells resembling Gaucher cells in the bone marrow, indicating glucocerebroside accumulation in these cells.

Table 1. Residual activities of lysosomal enzymes (nmol/hr/mg)

	White Blood Cells		Fibroblast		
	Patient	Control (n = 3)	Patient	Control (n = 3)	GD* Patient
glucocerebrosidase	7.4	49.1 ± 2.2	470.0	1757 ± 653	53
beta-galactosidase	210.1	234 ± 2.5	1135.0	1213 ± 529	1120
hexosaminidase	6085.0	7032.3 ± 901.3	33757.0	32760 ± 17225	20360

Abbreviation:
GD = Gaucher disease

In view of these observations, *N188S* may be a gene responsible for Gaucher disease. However, to reach a final conclusion, we should confirm glucocerebroside accumulation in tissues biochemically, as well as morphologic changes.

At least seven groups have reported on the *N188S* mutation in Gaucher disease, involving 16 patients in total. Among these 16 patients, four were free of neurologic signs. The *N188S* mutation was first suggested as a possible neuroprotective factor in Gaucher disease by Kim et al., in the way that the *N370S* mutation works in Caucasians [1]. Kim et al. [1] studied three patients with Gaucher disease: one *N188S* homozygote, and two siblings with *N188S/L444P*. At the time of that report, the three patients did not exhibit neurologic signs, and were diagnosed as manifesting type 1 Gaucher disease. Another Chinese patient with a diagnosis of type 1 Gaucher disease also manifested *N188S/L444P* [9]. However, more recent studies described *N188S* carriers who developed neurologic signs, including myoclonus [2,3,8-10]. For example, 4 of 16 patients with myoclonus carried *N188S* in a study by Park et al. [3]. Their genotypes were *N188S/RecNciI* (two patients), *N188S/84GG* (one patient), and *N188S*/recombinant allele (one patient). Another patient with myoclonus carrying *N188S* was reported by Filcamo et al. [4]; that patient was heterozygous with *S107L* [4]. All five patients presented general seizures as well as myoclonus, and four patients exhibited abnormalities in their electroencephalograms. Other reports described three patients whose seizures had not been specified [6,7]. Although the numbers of patients are too low to prove that *N188S* leads to myoclonus, the possibility should not be ignored. One speculation, based on documented cases, contends that when *N188S* is paired with a null mutation such as *D409H* or *RecNciI*, the phenotypes become severe, and this finding is not dependent on ethnicity. This correlation was also seen in our patient, who deteriorated progressively. She carries *N188S/G199D*, and *G199D* is a null mutation which has almost no enzyme activity. However, to support this speculation, it is necessary to follow the clinical courses of heterozygotes with *N188S* and null mutations, or *N188S* and mutations with a mild effect.

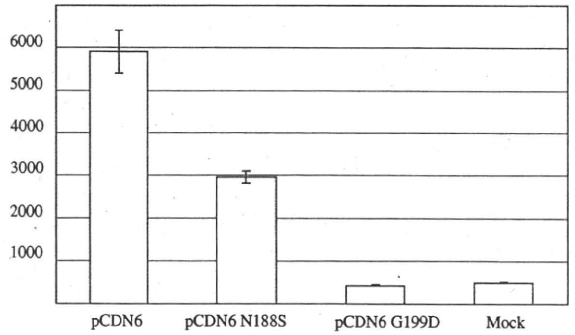

Figure 2. Glucocerebrosidase activity of the mutant proteins (nmol/hr/mg).

Montfort et al. suggested that the *N188S* mutation is a modifier variant [8]. They found three Spanish patients with a double mutant allele of *N188S* and *E326K*. In their in vitro study using a baculovirus expression system, the residual activity of *N188S+E326K* bearing glucocerebrosidase was lower than that of the *E326K*-bearing enzyme. The same effect was evident regarding *E326K* toward *N188S*. It is well-known that residual enzyme activity does not predict the severity of a phenotype in patients with Gaucher disease. However, the function of each mutation, and not residual activity, may affect the phenotypes of Gaucher disease. Therefore, more careful genetic analysis is important in detecting accurate genotypes of patients with Gaucher disease.

Our patient had manifested repeated exacerbations and remission of high fever without any clear signs of infection since age 18 years. Supranuclear gaze palsy was more distinct in the vertical position than in the horizontal position in this patient. The patient's cognitive ability may have been compromised. However, we think that the supranuclear gaze palsy had occurred horizontally and vertically. It would have been more informative if a biopsy had been available to detect any pathologic changes, as suggested by Conradi et al. [11]. The patient's central nervous system involvement progressed slowly, and her generalized convulsions increased. Unfortunately, she was unable to walk and became bedridden until her death at age 19 years.

In conclusion, we detected a novel mutation, *G199D*, with significantly low glucocerebrosidase activity. Although a correlation between *N188S* and myoclonus epilepsy cannot be established yet, it is strongly conceivable,

in light of our patient as well as previous reports. Moreover, the *N188S* mutation should be closely studied as a modifier gene that could affect the phenotype of a patient.

The authors thank Yoshikatsu Eto, MD, PhD, for his supervision, and Ms. Sayoko Iizuka for excellent technical assistance. This work was supported by a Grant for Research on Measures for Intractable Diseases from the Japanese Ministry of Health, Welfare, and Labor (2004-2006).

References

[1] **Kim** JW, Liou BB, Lai MY, Ponce E, Grabowski GA. Gaucher disease: Identification of three new mutations in the Korean and Chinese (Taiwanese) populations. Hum Mutat 1996;7:214-8.

[2] **Kowarz** L, Goker-Alpan O, Banerjee-Basu S, et al. Gaucher mutation *N188S* is associated with myoclonic epilepsy. Hum Mutat 2005;26:271-3.

[3] **Park** JK, Orvisky E, Tayebi N, et al. Myoclonic epilepsy in Gaucher disease: Genotype-phenotype insights from a rare patient subgroup. Pediatr Res 2003;53:387-95.

[4] **Filocamo** M, Mazzotti R, Stroppiano M, Grossi S, Dravet C, Guerrini R. Early visual seizures and progressive myoclonus epilepsy in neuronopathic Gaucher disease due to a rare compound heterozygosity (*N188S/ S107L*). Epilepsia 2004;45:1154-7.

[5] **Ida** H, Iwasawa K, Kawame H, Rennert OM, Maekawa K, Eto Y. Characteristics of gene mutations among 32 unrelated Japanese Gaucher disease patients: Absence of the common Jewish *84GG* and *1226G* mutations. Hum Genet 1995;95:717-20.

[6] **Ida** H, Rennert OM, Kawame H, Maekawa K, Eto E. Mutation prevalence among 47 unrelated Japanese patients with Gaucher disease: Identification of four novel mutations. J Inherit Metab Dis 1997;20:67-73.

[7] **Ida** H, Rennert OM, Iwasawa K, Kobayashi M, Eto Y. Clinical and genetic studies of Japanese homozygotes for the Gaucher disease *L444P* mutation. Hum Genet 1999;105:120-6.

[8] **Montfort** M, Chabas A, Vilageliu L, Grinberg D. Functional analysis of 13 GBA mutant alleles identified in Gaucher disease patients: Pathogenic changes and "modifier" polymorphisms. Hum Mutat 2004;23: 567-75.

[9] **Choy** FY, Zhang W, Shi HP, et al. Gaucher disease among Chinese patients: Review on genotype/phenotype correlation from 29 patients and identification of novel and rare alleles. Blood Cells Mol Dis 2007;38: 287-93.

[10] **Erdos** M, Hodanova K, Tasko S, et al. Genetic and clinical features of patients with Gaucher disease in Hungary. Blood Cells Mol Dis 2007;39:119-23.

[11] **Conradi** N, Kyllerman M, Månsson JE, Percy AK, Svennerholm L. Late-infantile Gaucher disease in a child with myoclonus and bulbar signs: Neuropathological and neurochemical findings. Acta Neuropathol (Berl) 1991;82:152-7.

Epilepsy & Seizure
Journal of Japan Epilepsy Society
Vol.3 No.1 (2010) pp.192-198

Epileptic focus in a case of subcortical band heterotopia: SISCOM and ictal EEG findings

Kenjiro Kikuchi, M.D. [1) 2)] Shin-ichiro Hamano, M.D. [1)], Fumihiro Goto, M.D.[1)], Akira Takahashi, R.T. [3)], Hiroyuki Ida, M.D. [2)]

[1]Division of Neurology, Saitama Children's Medical Center, 2100 Magome, Iwatsuki-ku, Saitama-city, Saitama 339-8551, Japan
[2]Department of Pediatrics, Jikei University School of Medicine, 3-25-8 Nishi-Shinbashi, Minato-ku, Tokyo 105-8471, Japan
[3]Department of Radiology, Saitama Children's Medical Center, 2100 Magome, Iwatsuki-ku, Saitama-city, Saitama 339-8551, Japan

Key words: antiepileptic drugs, carbamazepine, zonisamide, mechanism of action, calcium-induced calcium releasing systems

Published online November 10, 2010

Abstract

We presented an 11-month-old-girl with subcortical band heterotopia who had focal epilepsy detected by subtraction single photon emission computed tomography (SPECT) co-registered to magnetic resonance (MR) imaging (SISCOM) and ictal electroencephalogram. She manifested cluster of partial seizures composed of asymmetric tonic posturing accompanied by head rotation to the right side. Ictal electroencephalogram showed that paroxysmal discharges were generated from the right parieto-occipital area and spread to sur-

Corresponding author: Kenjiro Kikuchi, M.D., Division of Neurology, Saitama Children's Medical Center, 2100 Magome, Iwatsuki-ku, Saitama-city, Saitama 339-8551, Japan.
Phone: +81-48-758-1811; Fax: +81-48-758-1818; E-mail: kikuchi.kenjiro@pref.saitama.lg.jp

rounding areas. SISCOM revealed hyperperfusion in the overlying cortex of the right superior temporal gyrus, which corresponded to the onset area of ictal epileptiform discharges. These neurofunctional findings corresponded to her clinical seizures. Her seizures were controlled by high-dose phenobarbital therapy. We considered that the patient had focal epilepsy and that the epileptic focus might be in the overlying cortex, but not in the subcortical band.

Introduction

Subcortical band heterotopia (SBH) is a rare neuronal migration disorder, which shows ectopic gray matter separated from the overlying cortex by white matter. Patients with SBH have been reported to have intractable epilepsies and mental retardations [1, 2]. These patients may present with either generalized epilepsies or focal epilepsies [2]. The epilepsies are usually evaluated by ictal and/or interictal electroencephalogram (EEG), and are rarely diagnosed by ictal single photon emission computed tomography (SPECT) or subtraction ictal SPECT coregistered to magnetic resonance (MR) imaging (SISCOM). To our knowledge, there are no reports on SISCOM evaluation of SBH during infancy. Here we report an 11-month-old girl with SBH who was diagnosed with focal epilepsy by SISCOM and ictal EEG.

Case report

An 11-month-old girl was admitted to our hospital because of intractable seizures persisting for 2 weeks. The perinatal and familial histories of the patient were unremarkable. Neurological examinations showed hypotonia in her lower extremities. She was able to sit by herself at 10 months, but could not crawl or stand up by herself at that time. Her seizures were characterized by asymmetric tonic posturing for 30 seconds accompanied by head rotation to the right side, which occurred 4 to 6 times per day.

Interictal EEG demonstrated irregular spike-and-waves and 3-4 Hz high-voltage slow waves (HVS) in the left centro-parieto-occipital area. As background EEG activities, low amplitude (20-30 μV) fast waves (30 Hz) were found in the right hemisphere. Brain MRI revealed a thin overlying cortex and an excessive band of subcortical gray matter, which was split by white matter from the frontal to the occipital region (Fig. 1). Bilateral occipital cortical surfaces were smooth and agyri. These abnormal findings were compatible with diffuse subcortical band heterotopia. Mutation in the DCX gene (178A>G) was found in exon 2.

Her seizure frequencies increased from 4-6 times per day to 4-5 times per hour, despite treatment with valproate. Ictal EEG demonstrated 3-4 Hz high-voltage slow (HVS) waves and sharp waves in the left centro-parieto-temporal area, which subsided and then 14-15 Hz fast activities with 90 μV amplitude appeared in the right mid-temporal area (Fig. 2A). These fast discharges propagated to surrounding areas and their amplitude

increased (Fig. 2B). They were followed by 5-6 Hz high voltage polymorphic discharge burst for about 20 seconds (Fig. 2C), and then 1-2 Hz HVS waves in the right hemisphere for 40 seconds (Fig. 2D). Finally these 1-2 Hz HVS discharges terminated and sharp waves reappeared in left centro-temporal area, similar to the interictal EEG findings mentioned above (Fig. 2E). The total duration of ictal activities was 75 seconds. Clinical manifestation of her seizures was recognized 30 seconds after the 14-15 Hz fast activities appeared.

Technetium-99m-ethyl cysteinate dimmer (ECD) was used for ictal SPECT. The patient was injected with 185 MBq 99m-Tc-ECD immediately after clinical seizure began, and the seizures lasted for 45 seconds after ECD injection. After ictal SPECT examination, she was given high-dose phenobarbital (PB) therapy by rectal suppository at an initial dose of 30 mg/kg/day for the first two days, followed by a dose of 20 mg/kg/day for 2 days, 10 mg/kg/day for 2 days, then 10 mg/kg/day by oral administration for the sequential consecutive days. Her seizures disappeared after PB therapy.

Interictal ECD-SPECT was performed after the disappearance of seizures. To elucidate the ictal hyperperfusion regions, we used the SISCOM analysis. The SISCOM images demonstrated hyperperfusion in the overlying cortex of the right superior temporal gyrus (Fig. 3), which corresponded to ictal EEG findings.

The patient had no seizures for more than 3 months after high-dose PB therapy, and was able to crawl and stand up by herself at the last follow-up.

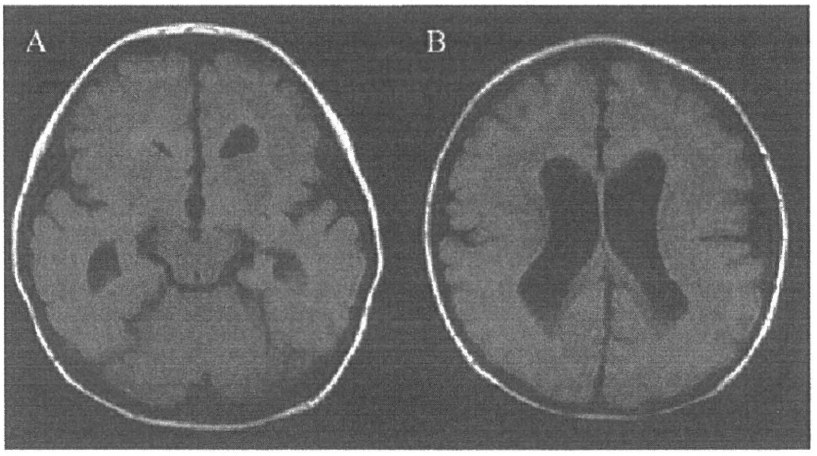

Fig. 1. Axial T1-weighted magnetic resonance (MR) imaging

Axial T1-weighted images show diffuse subcortical heterotopic gray matter and mild pachygyria.

A. At the level of cerebral peduncle.

B. At the level of body of the lateral ventricle.

Discussion

We performed SISCOM and ictal EEG on an infant with SBH. Ictal EEG indicated that the ictal paroxysmal discharges originated from the right temporal region. SISCOM showed that the hyperperfusion area corresponded to the site of onset of ictal paroxysmal discharges, and that this hyperperfusion area seemed to be corresponded to the overlying cortex of the right superior temporal gyrus. To our knowledge, this is the first report of SISCOM analysis in infant with SBH.

Some experimental studies in SBH rat models reported the correlation between

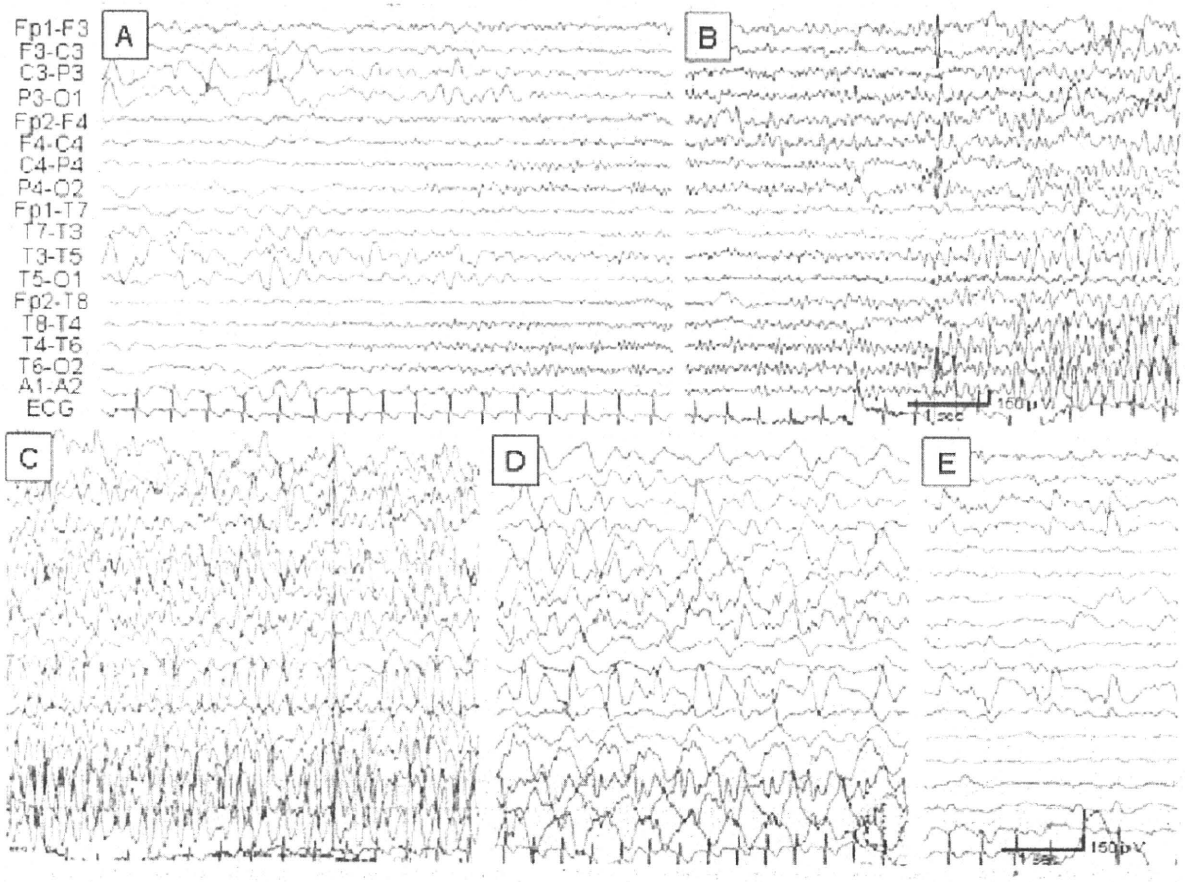

Fig. 2. Ictal electroencephalogram at the age of 11 months

(A) 3-4 Hz high-voltage slow (HVS) waves and sharp waves are found in the left centro-parieto-temporal area. The HVS disappeared and burst of 14-15 Hz fast waves is observed in the right mid-temporal area.

(B) At 10 seconds after onset, fast waves have generalized and the amplitude increases.

(C) At 15 seconds after onset, 5-6 Hz high voltage polymorphic discharges burst for about 20 seconds.

(D) From 35 seconds after onset, 1-2 Hz HVS waves in the right hemisphere persist for 40 seconds.

(E) At 75 seconds after onset, HVS waves terminate and sharp waves remain in the left centro-temporal area.

overlying cortex and subcortical band. Chen et al. [3] concluded that normotopic neurons were responsible for initiating seizures in the dysplastic neocortex, because normotopic neurons were more likely to exhibit epileptiform activity than heterotopic neurons, and heterotopic neurons were recruited into spiking by activity initiated in normotopic neurons. These observations are consistent with our findings.

Ictal SPECT has the potential to localize the ictal onset zone accurately in a noninvasive manner, and is particularly useful in MRI-negative localized epilepsy and focal cortical dysplasias [4]. Furthermore, SISCOM is useful to define the onset site of seizure [5, 6]. To our knowledge, this is the first report of SISCOM finding of SBH in infant. SISCOM images showed that the hyperperfusion area corresponded to the onset region of the ictal EEG discharges, and that this region was located in the overlying cortex. These results show that the overlying cortex may be the epileptic focus in our SBH patient.

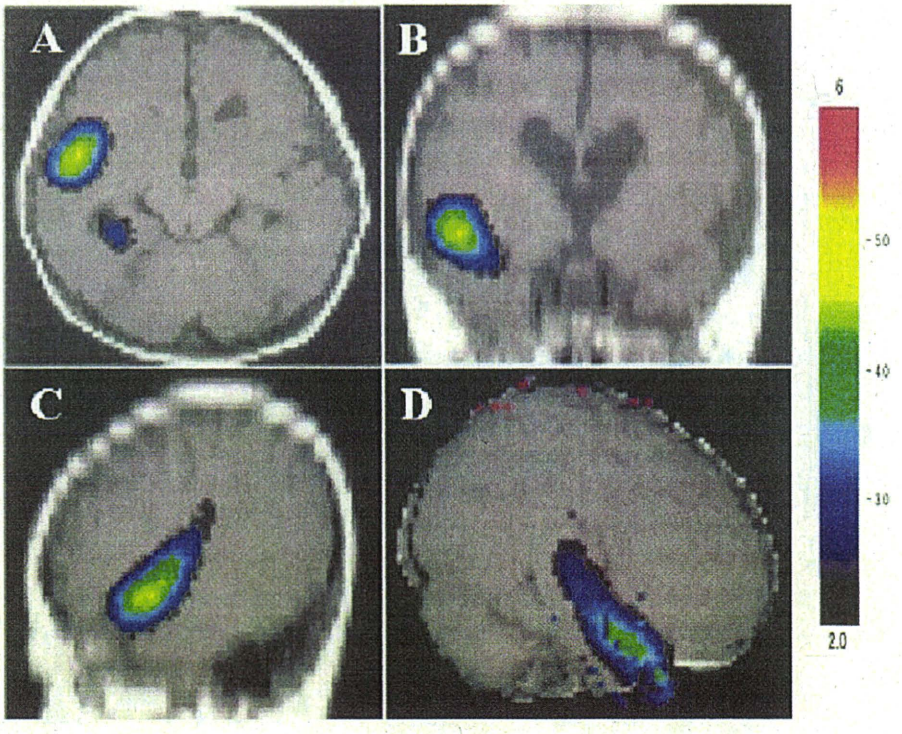

Fig 3. Subtraction ictal single-photon emission computed tomograpghy (SPECT) coregistered to magnetic resonance (MR) imaging (SISCOM)

(A) In axial view, hyperperfusion is observed in the right frontotemporal area and right medial occipitotemporal area. (B) Coronal view. (C) Sagittal view. (D) Right lateral view. (B)-(D) show that hyperperfusion is located in the right superior temporal gyrus.

Surgical treatment has been performed on focal epilepsy patients with SBH. Bernasconi et al. [7] reported that five of eight patients had no significant improvement by surgical treatment and that temporal resection resulted in especially poor outcome. They suggested that SBH might have a multifocal generator due to widespread structural abnormality, even though clinical and neurofunctional studies proved the existence of focal epileptogenic lesions. Mai et al. [8] reported that one patient with SBH had good outcome by resection of the posterior third of the middle and inferior temporal gyri and part of the fusiform gyrus. However, both groups could not explain the mechanism of seizure generation related to the normal overlying cortex and the subcortical band. Our findings suggest that surgical treatment including corticectomy will be a therapeutic option for patients with SBH.

We demonstrated symptomatic focal epilepsy using SISCOM and ictal EEG in a pediatric patient with SBH, and speculated that the overlying cortex may be the epileptic focus.

Acknowledgement

We would like to thank Dr. Mitsuhiro Kato (Yamagata University School of Medicine) for analyzing the DCX gene, and Emeritus Professor Eric Johnson (Jichi Medical University, Tochigi, Japan) for his assistance with the preparation of the manuscript.

References

[1] Barkovich AJ, Guerrini R, Battaglia G, Kalifa G, N'Guyen T, Parmeggiani A, Santucci M, Giovanardi-Rossi P, Granata T, D'Incerti L. Band heterotopia: correlation of outcome with magnetic resonance imaging parameters. Ann Neurol 1994;36:609-17.

[2] Palmini A, Andermann F, Aicardi J, Dulac O, Chaves F, Ponsot G, Pinard JM, Goutières F, Livingston J, Tampieri D, Andermann E, Robitaille Y. Diffuse cortical dysplasia, or the 'double cortex' syndrome: The clinical and epileptic spectrum in 10 patients. Neurology 1991;41:1656-62.

[3] Chen ZF, Schottler F, Bertram E, Gall CM, Anzivino MJ, Lee KS. Distribution and initiation of seizure activity in a rat brain with subcortical band heterotopia. Epilepsia 2000;41:493-501.

[4] Van Paesschen W. Ictal SPECT. Epilepsia 2004;45(Suppl.4):35-40.

[5] O'Brein TJ, So EL, Mullan BP, Hauser MF, Brinkmann BH, Bohnen NI, Hanson D, Cascino GD, Jack CR, Sharbrough FW. Subtraction ictal SPECT co-registered to MRI improves clinical usefulness of SPECT in localizing the surgical seizure focus. Neurology 1998; 50:445-54

[6] Véra P, Kaminska A, Cieuta C, Hollo A, Stiévenart JL, Gardin I, Ville D, Mangin JF, Plouin P, Dulac O, Chiron C. Use of subtraction ictal SPECT co-registered to MRI for optimizing the localization of

seizure foci in children. J Nucl Med 1999;40:786-92

[7] Bernasconi A, Martinez V, Rasa-Neto P, D'Agostino D, Bernasconi N, Berkovic S, MacKay M, Harvey AS, Palmini A, Costa da Costa J, Paglioli E, Kim HI, Connolly M, Olivier A, Dubeau F, Andermann E, Guerrini R, Whisler W, de Toledo-Morrell L, Morrell F, Andermann F. Surgical resection for intractable epilepsy in 'double cortex' syndrome yields inadequate results. Epilepsia 2001;42:1124-9.

[8] Mai R, Tassi L, Cossu M, Francione S, Lo Russo G, Garbelli R, Ferrario A, Galli C, Taroni F, Citterio A, Spreafico R. A neuropathological, stereo-EEG, and MRI study of subcortical band heterotopia. Neurology 2003;60:1834-8.

症例報告

Key Words：
ジストニア、瀬川病、尖足、ドーパ、
歩行障害

脊髄疾患、心因反応が疑われていた瀬川病の女児例－鑑別点とその病態

日暮憲道[1]、浜野晋一郎[1]、田中　学[1]、大場温子[1]、
黒田直宏[1]、吉成　聡[1]、南谷幹之[2]

要　旨

瀬川病は小児期に著明な日内変動を呈する下肢の姿勢ジストニアで発症する常染色体優性遺伝性疾患である。L-dopaが著効するが、比較的稀な疾患であり正しく診断されていないことも多い。今回我々は、7歳時に右側に尖足が出現し、その後左側へも広がり歩行障害を呈し、当初脊髄疾患など他疾患が疑われていた11歳女児例を経験した。症状は朝に軽度で、時間とともに増悪する日内変動が認められた。下腿に筋萎縮のない強剛様の筋緊張亢進を認め、足関節は拘縮なく他動的に背屈可能で関節可動域制限なく、ジストニアと考えられた。瀬川病を疑いL-dopa単剤治療を開始したところ症状は順調に消失した。髄液プテリジン分析ではビオプテリン、ネオプテリンの著明な低値が認められた。本疾患は治療有効性から早期診断、早期治療開始が大変重要である。症例の考察とともにその病態に関して報告する。

はじめに

ジストニアは主力筋と拮抗筋の持続的な共収縮により異常姿勢を呈する症候である[1]。瀬川病は小児期に著明な日内変動を呈するジストニアを主徴とする疾患である。少量のL-dopaによって劇的に症状改善を示すが、発症後数年以上にわたり診断されず、長期臥床の生活を強いられることも稀ではない[2]。今回我々は、当初脳性麻痺や脊髄疾患、心因などが疑われた瀬川病の女児例を経験した。治療効果の面から、その診断は患者のQOLを大きく左右する問題であるため、鑑別の注意点や病態に関して報告する。

症　例

【症例】11歳女児

【主訴】両側下肢の内反尖足、歩行障害

【既往歴】妊娠経過順調で仮死なく出生、その後成長・発達は正常

【家族歴】特記すべきことなし

【現病歴】7歳の頃に右足の内反尖足が出現した。症状はその後両側へ広がり、歩行障害も認められるようになった。脳外科で脊髄係留症候群などの脊髄疾患が疑われ、脊髄MRI、膀胱内圧測定、腎シンチグラフィーが行われたが異常は認められなかった。整形外科の診察でも異常は認められず、10歳1ヶ月時に当科紹介受診した。その際、バビンスキー反射は認めなかったが、膝蓋腱反射の軽度亢進が認められた。脳性麻痺による尖足、ミオパチー、重症筋無力症による垂れ足が疑われたが、頭部MRI、MRアンギオグラフィー、反復誘発筋電図、抗アセチルコリン受容体抗体価に異常は認められなかった。心理的な要因も考えられ心療内科や心理外来での経過観察も行われたが、その後も症状は進行した。症状は朝には軽く、自力歩行が可能なことも多かったが、昼から夜にかけて、あるいは運動後など疲労時に増悪する傾向が認められた。11歳1ヶ月時には夜間は四つ這いで移動する状態であり、精査加療目的で当科入院となった。

【入院時現症】体重38.6kg (+0.24SD)、身長143.8cm

埼玉県立小児医療センター　神経科[1]、保健発達部[2]

(+0.05SD)。意識清明で、発語、会話や知的状態は正常。両側足関節の内反尖足を認める。下腿は強剛様筋緊張亢進を認める。足関節の他動的背屈は可能で、関節可動域制限は認めない。膝蓋腱反射の亢進やバビンスキー徴候、クローヌスなど錐体路徴候を認めない。症状は両側下腿に限局し、他部位には認めない。その他一般的身体所見、神経学的所見の異常を認めない。

【入院時検査成績】血算、一般的生化学検査所見に異常を認めない。髄液一般検査所見に異常なし。乳酸、ピルビン酸は血液、髄液ともに異常なし。血清カルニチン分画、ミオグロビンは正常。髄液ネオプテリンは1pmol/ml以下（測定感度以下）。血中アミノ酸分析はフェニルアラニンを含め正常。尿アミノ酸分析でシスチン尿症の所見を認める。

【経過】下腿の筋萎縮や錐体路徴候、足関節の拘縮は認めず、下腿三頭筋と前脛骨筋に強剛様の持続的筋収縮が認められ、これらの特徴からジストニアが考えられた。尖足は起床直後には軽度で短距離であれば自力歩行が可能であったが、軽度の運動によって悪化し歩行は困難となった。また、症状は夕から夜にかけて増強した。運動による増悪と日内変動が明らかで、他の神経所見に異常は認めず、症状や経過、発症年齢から瀬川病が考えられた。入院10日目よりレボドパ（ドパール®）内服を100 mg/日より開始した。数日毎に増量し、600 mg/日の内服から症状は明らかな改善傾向を認めた。しかし、跛行は軽度残存し短時間で疲労し、夜には尖足が増強したため、入院21日目より800 mg/日へ増量し退院となった。幻覚やジスキネジアなどの副作用は認めなかった。治療開始前に採取した検体で、他施設で測定したプテリジン分析の結果は、ネオプテリン、ビオプテリンはそれぞれ血液で2.1 nM（対照平均±SD:17.9±10.6、以下同じ）、12.5 nM (24.6±5.9)、髄液で5.4 nM (8.0-25.0)、4.0 nM (10.0-20.0)と著明な低値であり、瀬川病として矛盾のない結果であった。退院後症状は消失し、レボドパは500mg/日へ減量したが寛解が持続している。怠薬で症状は再燃するが、内服が十分であれば運動障害は消失している。

考　察

瀬川病は、1971年に瀬川らによって最初に報告され、1976年に初めて“著明な日内変動を呈する遺伝性進行性ジストニー”の病名で記載された[3]。通常4-8歳で一側下肢に内反尖足を呈するジストニア姿勢で発症し、両側下肢、さらに四肢へ広がる進行性の経過をたどる4)。女性に多く、進行は10歳代には速いが、20歳代には緩徐となり、30歳代には停止する。約8割の症例で朝に軽く夜へ向かい悪化する日内変動を認める。しかし、上肢のジストニア運動を呈する症例や、特に成人発症例では日内変動や進行を認めないため、多彩な臨床像を呈する。診断は特徴的臨床症状に加え、髄液中のビオプテリン、ネオプテリンの低下、白血球中のGuanosine triphosphate cyclohydrolase- I (GCH)活性の低下（後述）を検査することが勧められるが、検査が可能な施設が限定されることからL-dopa投与による診断的治療を行うことも実際的である。L-dopa単剤で20 mg/kg/日、カルビドパ合剤で4-5 mg/kg/日で多くは症状寛解が得られる。また、現在では約60-80%の症例で遺伝子診断が可能である。

本症例は瀬川病に典型的な経過であったが、本疾患は症状の多様性や疾患の稀少性から、典型例においても正しく診断されていない例は少なくない[2]。瀬川病ではしばしば腱反射亢進やクローヌスを伴うことがあるため、ジストニアではなく痙性麻痺として捉えられ、脳性麻痺や脊髄障害などと診断されていることが少なくない[5]。本症例でも当初は腱反射亢進が認められ、脊髄疾患が疑われた。しかし、striate toe signに伴う母趾背屈が認められることはあるものの、バビンスキー兆候は認めず、強剛様筋緊張亢進で筋萎縮はなく、錐体路障害とは異なる性質を持つ。さらに多くの例で日内変動が明らかであり、必ず確認する必要がある。本疾患の大半の症例では少量のL-dopaで症状が消失し、適切な投与量ではドーパ誘発性ジスキネジアやwearing-off現象などの副作用がなく、その効果が永続することも特徴である。また、本症例では認めなかったが、小児期発症例では長期に放置されることによって低身長を来すことがある。これもL-dopaで予防可能である。このため本疾患では、早期診断、早期治療が大変重要であり、診断と治療開始の遅れが患者のQOLに与える影響は大きい。

瀬川病の主な原因は、14q22.1-q22.2に存在するGCH遺伝子の異常である[6]。常染色体優性遺伝を呈し、ヘテロ異常によるGCH部分欠損により、活性が20%未満になると発症するとされている。GCHはTyrosine hydroxylase (TH) の補酵素である

Tetrahydrobiopterin (BH4) 合成の律速酵素であり、GCH の活性低下によって BH4 合成過程の基質が減少し、ビオプテリン、ネオプテリンが低下する（図 1)。また、BH4 は TH 以外にセロトニン合成に必要な Tryptophan hydroxylase の補酵素でもあるが、複合ヘテロ接合体では GCH 活性低下がより強く、セロトニン欠乏の症状（運動発達遅滞、体幹筋緊張低下）を伴う[7]。このため、複合ヘテロ接合体患者では、脳性麻痺など非可逆性の疾患と誤診される可能性がより高く、注意を要する。本症例では入院時、髄液ネオプテリン値の著明な低下を認め、その後の診断プロセスや、早期の診断的治療の介入に有用であった。ネオプテリンは検査会社での測定が可能であり、原因不明の筋緊張亢進を認めた場合には測定する価値がある。

瀬川病の発症年齢、症状、進行などの病態には、大脳基底核の機能が思春期を境に大きく変化することが影響していると考えられている[8]。線条体の発達は、直接路に関与するドパミン（DA）-D1 受容器を持つ細胞が分布する腹側部から、間接路に関与する DA-D2 受容器を持つ細胞が分布する背側の順に成熟する。従って、小児期には間接路の発達は未熟で、主に直接路が病態に関与する。一方、大脳基底核出力系は脳幹網様体脊髄路に向かう下行性経路が早期に発達し、視床から大脳皮質へ向かう上行性経路の発達は遅れる[9]。さらに、黒質線条体 DA ニューロン終末における TH 活性は小児期に高く、10-15 歳の間に急激に低下し、20 歳代前半から成人レベルに達する 8)。これらの背景から、瀬川らは病態を以下のように明解に説明している 4)。幼児期前半は TH 活性が高く DA 欠乏が目立たないが、学童期から思春期にかけての TH 活性の低下に伴い、線状体 DA 欠乏が顕在化する。黒質緻密質から D1 線条体直接路に対する促通作用が低下し、線条体の淡蒼球内節・黒質網様質に対する抑制作用が減弱する（図 2)。この時、視床や、歩行に重要な脚橋核の活動は抑制されておらず、歩行機能は障害されない。しかし、網様体脊髄路が過剰に抑制されるため、下肢に姿勢ジストニアとして尖足症状を発症する。その後、上行路の発達に伴い、黒質緻密質 DA ニューロンから視床下核 D1 受容器を介する入力[10]が減弱し、視床下核が抑制され、淡蒼球内節に対する促通作用が減弱し、視床皮質路の脱抑制を生じ、姿勢ジストニアとは異なる動作性ジストニアや振戦が出現する。従って、思春期以降の発症では小児期と異なり、間接路、上行性経路を基盤とした症状が出現すると考えられている。さらに、L-dopa 内服前の小児に合併する低身長は、灰白隆起漏斗路 D4 受容体へ投射する DA ニューロンの活性低下と関連すると考えられている。

本症例では、瀬川病の疾患概念の理解、問診、注意深い診察により、本疾患を疑うことは可能であった。瀬川病を含めドーパ反応性ジストニアは、薬物による

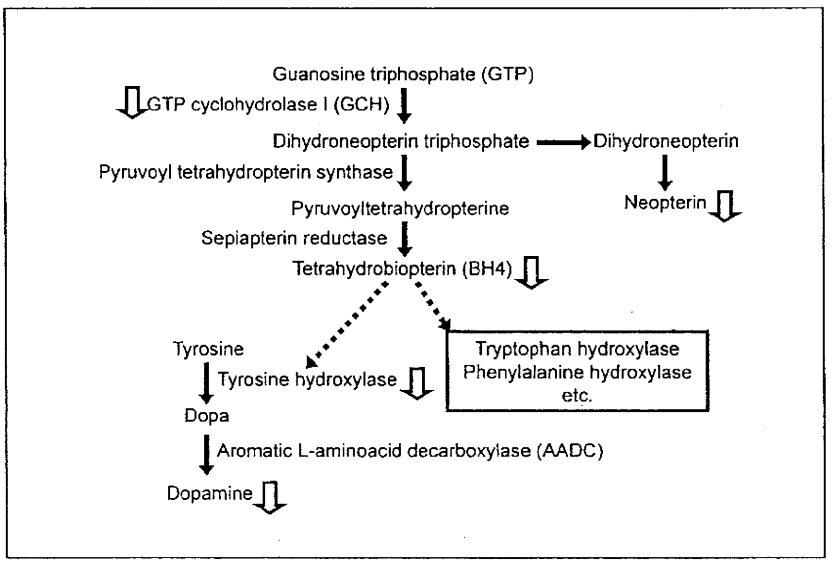

図 1 Tetrahydrobiopterin、Dopamine 合成の代謝経路の概略

波線矢印は補酵素としての関与を示す。白抜き下向き矢印は瀬川病の病態に関わる代表的変化を示す。
GTP cyclohydrolase I の低下が最初の変化となる。

治療効果と、それが患者のQOLに与える影響は絶大である。非典型例も多く、原因不明の筋緊張亢進を呈する疾患では、本疾患を考慮する必要がある。特に尖足で発症するため、痙性を呈する脳性麻痺、脊髄疾患などと診断されやすいことは銘記すべきである。

謝辞　稿を終えるにあたり，血清および髄液、尿のプテリジン分析を行って頂いた大阪市立大学大学院医学研究科発達小児医学の新宅治夫先生に深謝いたします。

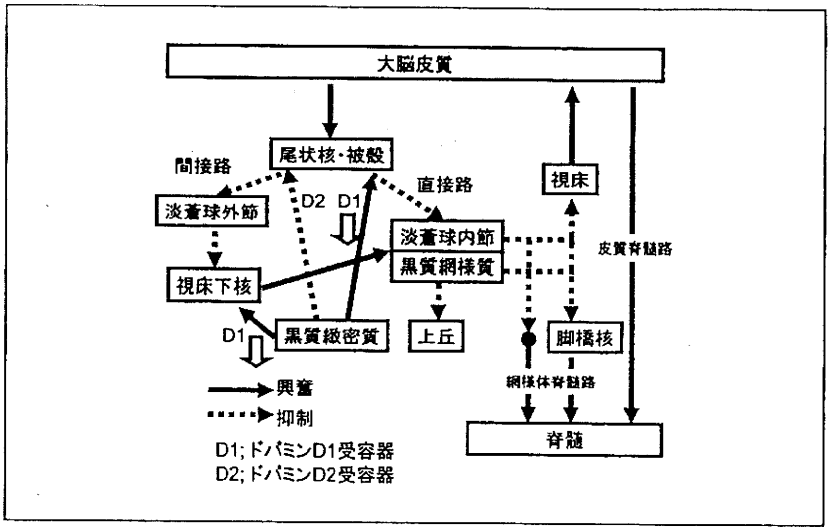

図2　大脳基底核の回路図

黒質緻密質のドパミンニューロンは線条体、視床下核へ入力しており、D1受容器は促通性、D2受容器は抑制性の調節を担っている。その他のニューロンでは主にグルタミン酸が促通性、γアミノ酪酸(GABA)が抑制性の調節を行っている。瀬川病では白抜き下向き矢印で示す部分で、ドパミンD1受容器を介す促通作用の減弱が生じている。

参考文献

1）Fahn S, Marsden CD, Calne DB: Classification and investigation of dystonia. Movement disorders. Butterworths, London, 332-358, 1987

2）Jan MMS: Misdiagnoses in children with dopa-responsive dystonia. Pediatr Neurol 31 : 298-303, 2003

3）Segawa M, Hosaka A, Miyagawa F, Nomura Y, Imai H: Hereditary progressive dystonia with marked diurnal fluctuation. Advances in neurology. Vol 14. Raven Press, New York, 215-233, 1976

4）瀬川昌也：瀬川病. Brain Nerve 60:5-11, 2008

5）Nygaard TG, Waran SP, Levine RA, et al.: Dopa-responsive dystonia simulating cerebral palsy. Pediatr Neurol 11:236-240, 1994

6）Segawa M, Nomura Y, Nishiyama N: Autosomal dominant guanosine triphosphate cyclohydrolase I deficiency (Segawa disease). Ann Neurol 54(Suppl 6):S32-S45, 2003

7）Furukawa Y, Kish SJ, Bebin EM, et al.: Dystonia with motor delay in compound heterozygotes for GTP-cyclohydrolase I gene mutations. Ann Neurol 44:10-16, 1998

8）野村芳子：不随意運動の臨床－小児例－. 脳と発達 29:199-205, 1997

9）島史雄，石堂克哉，加藤元博：不随意運動と大脳基底核遠心路－ジストニーに対する定位脳手術の経験から－. 脳と発達 29:206-212, 1997

10）Kreiss DS, Mastropietro CW, Rawji SS, et al.: The response of subthalamic nucleus neurons to dopamine receptor stimulation in a rodent model of Parkinson' s disease. J Neurosci 17:6807-6819, 1997

A case with Segawa disease—A often misdiagnosed disease and its pathophysiology

Norimichi Higurashi[1], Shin-ichiro Hamano[1], Manabu Tanaka[1], Atsuko Oba[1], Naohiro Kuroda[1], Satoshi Yoshinari[1], Motoyuki Minamitani[2]

[1]Division of Neurology and [2] Division of Child Health and Human Development, Saitama Children's Medical Center

We report here a girl patient with Segawa disease. Her initial symptom was equines foot in the right appeared at the age of 7. Subsequently, the symptom also developed in the left, resulted in gait disturbance. She was initially suspected as having spinal cord disease or psychological problems, and correct diagnosis had not been made for a few years. When she was hospitalized at the age of 11, she presented gait disturbance with bilateral leg stiffness and equinus posture. However, spasticity, muscle atrophy and joint contracture were not observed in her legs. Her symptoms were mild in the morning, but worsened later in the day. We suspected Segawa disease because of her typical dystonic symptoms and decreased neopterin concentration in her cerebrospinal fluid. L-dopa dramatically alleviated her symptoms. Segawa disease is a dominantly-inherited disease characterized by progressive dystonia with diurnal fluctuation and dramatic responsiveness to L-dopa. Misdiagnosis is not uncommon because of its rarity and similarity of symptoms to spastic plegia. Early diagnosis of this treatable disease is important for reducing suffering of the patients.

Epilepsy Research (2010) 88, 100–107

ELSEVIER

journal homepage: www.elsevier.com/locate/epilepsyres

MEG time–frequency analyses for pre- and post-surgical evaluation of patients with epileptic rhythmic fast activity

Keitaro Sueda[a], Fumiya Takeuchi[b], Hideaki Shiraishi[a], Shingo Nakane[c], Naoko Asahina[a], Shinobu Kohsaka[a], Hideyuki Nakama[d], Taisuke Otsuki[d], Yutaka Sawamura[e], Shinji Saitoh[a,*]

[a] *Department of Pediatrics, Hokkaido University Graduate School of Medicine, North 15 West 7, Kita-ku, Sapporo, 060-8638, Japan*
[b] *Department of Health Science, Hokkaido University School of Medicine, Japan*
[c] *Division of Magnetoencephalography, Hokkaido University Hospital, Japan*
[d] *Department of Neurosurgery, Musashi Hospital, National Center of Neurology and Psychiatry, Japan*
[e] *Department of Neurosurgery, Hokkaido University Graduate School of Medicine, Japan*

Received 4 April 2009; received in revised form 21 September 2009; accepted 4 October 2009
Available online 6 November 2009

KEYWORDS
Magnetoencephalography;
Fast activity;
Fourier transform;
Time–frequency analysis;
Symptomatic localization-related epilepsy;
Surgical evaluation

Summary
Purpose: To evaluate the effectiveness of surgery for epilepsy, we analyzed rhythmic fast activity by magnetoencephalography (MEG) before and after surgery using time–frequency analysis. To assess reliability, the results obtained by pre-surgical MEG and intraoperative electrocorticography were compared.
Methods: Four children with symptomatic localization-related epilepsy caused by circumscribed cortical lesion were examined in the present study using 204-channel helmet-shaped MEG with a sampling rate of 600 Hz. One patient had dysembryoplastic neuroepithelial tumor (DNT) and three patients had focal cortical dysplasia (FCD). Aberrant areas were superimposed, to reconstruct 3D MRI images, and illustrated as moving images.
Results: In three patients, short-time Fourier transform (STFT) analyses of MEG showed rhythmic activities just above the lesion with FCD and in the vicinity of DNT. In one patient with FCD in the medial temporal lobe, rhythmic activity appeared in the ipsilateral frontal lobe and temporal lateral aspect. These findings correlate well with the results obtained by intraoperative electrocorticography. After the surgery, three patients were relieved of their seizures, and the area of rhythmic MEG activity disappeared or become smaller. One patient had residual rhythmic MEG activity, and she suffered from seizure relapse.

* Corresponding author. Tel.: +81 11 706 5954; fax: +81 11 706 7898.
E-mail address: ss11@med.hokudai.ac.jp (S. Saitoh).

0920-1211/$ – see front matter
doi:10.1016/j.eplepsyres.2009.10.002

Conclusion: Time–frequency analyses using STFT successfully depicted MEG rhythmic fast activity, and would provide valuable information for pre- and post-surgical evaluations to define surgical strategies for patients with epilepsy.

Introduction

Magnetoencephalography (MEG) is applied to localize the source of epileptiform discharges in patients with refractory epilepsy, particularly in symptomatic localization-related epilepsy, as it is noninvasive and exhibits excellent temporal and spatial resolution. MEG is a predictive tool for epileptic surgery. MEG localization of epileptiform discharges has been successfully achieved by single dipole modeling (SDM), which is mainly used to analyze interictal epileptiform spikes (Hämäläinen et al., 1993; Ebersol, 1997). However, the application of SDM appears to be limited to patients with localized spikes, since the algorithm is based on the presumption that the current epileptic discharge originates from a single spot.

Rhythmic electroencephalography (EEG) activities are often the hallmarks of underlying epileptogenesis. Rhythmic polyspike activities have been reported as indicative of an irritative epileptogenic zone in the electroencephalography (Gambardella et al., 1996). A scalp EEG showed interictal focal paroxysmal beta activity in children with epilepsy caused by brain tumor, arteriovenous malformation, and cystic lesion (Hooshmand et al., 1980). In surveys of surgical outcomes, the locations of ictal rhythmic beta activities on scalp EEG and intracranial EEG have been correlated with the onset of seizures in patients with neocortical epilepsies (Talairach et al., 1992; Lee et al., 2000; Park et al., 2002; Worrell et al., 2002; Bonati et al., 2006). However, the resolution of EEG is not powerful enough to properly evaluate rhythmic activity because EEG activity is affected by the conductivity of brain structures (Hämäläinen et al., 1993), and in some cases EEG is unable to detect notable pathological activity (Iwasaki et al., 2005).

Recently, time–frequency analyses of EEG and MEG have been used to investigate rhythmic activities (Haykin et al., 1996; Grosse et al., 2002; Bosnyakova et al., 2006). Short-time Fourier transform (STFT) applies a short-time window to the signal and performs a series of Fourier transforms within this window as it slides across the recorded data (Oppenheim and Schafer, 1999). This technique can be used to estimate the time–frequency components of the signal and visualize the spectral distributions. It has been proposed to apply this technique to patients with epilepsy (Kiymik et al., 2005), as it provides temporal changing information on the time–frequency domain.

Our current study was conducted to evaluate the effectiveness of surgery for epilepsy using pre- and post-operative MEG to assess changes in epileptic rhythmic activity.

Patients and methods

Patients

Four children with refractory symptomatic localization-related epilepsy induced by a circumscribed cortical lesion were enrolled in the present study. They underwent surgery between September 2005 and April 2008. Their guardians gave written informed consent for this study.

Methods

MEG

MEG data before and after surgery were recorded using a 204-channel helmet-shaped neuromagnetometer (Neuromag Vectorview; Elekta-Neuromag Oy, Stockholm, Sweden) with pairs of orthogonal planar gradiometers at 102 locations. The recordings were carried out in a magnetically shielded room, with the patient in a supine position. The MEG data were collected for about 40 min for each patient at a sampling rate of 600 Hz. During the MEG examination, Patients 1, 2 and 4 received intravenous sodium thiopental for sedation, to avoid motion artifacts, while Patient 3 did not require sedation. A scalp EEG was recorded simultaneously using the international 10-20 system.

MEG data analysis. MEG data were filtered for offline analysis with a band pass of 3–100 Hz.

The segments that contained abnormal paroxysms were selected manually. Single spikes were analyzed by SDM, to determine the distribution of brain activity generating the spike. Rhythmic fast activity discharges were analyzed by STFT, to determine the localization and value of each selected discharge.

SDM. The dipole-fit software (Neuromag, Helsinki, Finland) was used to calculate the equivalent current dipoles (ECDs). We defined acceptable ECDs as having goodness of fit (GOF) >70% and ECD strength of between 100 and 800 nAm. GOF is a measure of how well the ECD model explains the measured signals. Acceptable ECDs were superimposed on the MRIs.

STFT analysis. STFT was used to reveal the distributions of MEG fast activity (Oppenheim and Schafer, 1999) and the MATLAB (MathWorks, Natick, MA, USA) program was used to execute the STFT for the MEG signals. Each signal was divided into small sequential frames, and fast Fourier transformation (FFT) was applied to each frame.

In the present study, the STFT was implemented using a 256-point window. The time of each window was 426.7 ms (i.e., 256 points × 1000 ms/600 Hz). The window was shifted every four points, which corresponded to 6.7 ms (i.e., 1000 ms/600 Hz × 4 points). FFT was applied to each window. This process was repeated for the whole signals that were selected. The time–frequency distributions are displayed as graphs (Fig. 2C).

A spectrum was considered to be aberrant when it was observed in the graph to be isolated from the background frequency spectrum. An aberrant frequency spectrum on the graph was superimposed onto the reconstructed 3D MRI.

ECoG

The ECoG studies were performed during surgery. The ECoG data were collected using the Ceegraph system (Bio-Logic, Mundelein, IL, USA), with a sampling rate of 512 Hz. A 4 × 5 grid electrode array was used for Patients 1 and 4. A 4 × 8 grid electrode array was used for Patient 3. A four-channel strip electrode was used for Patient 2. Recording was performed for at least 1 min at each electrode location.

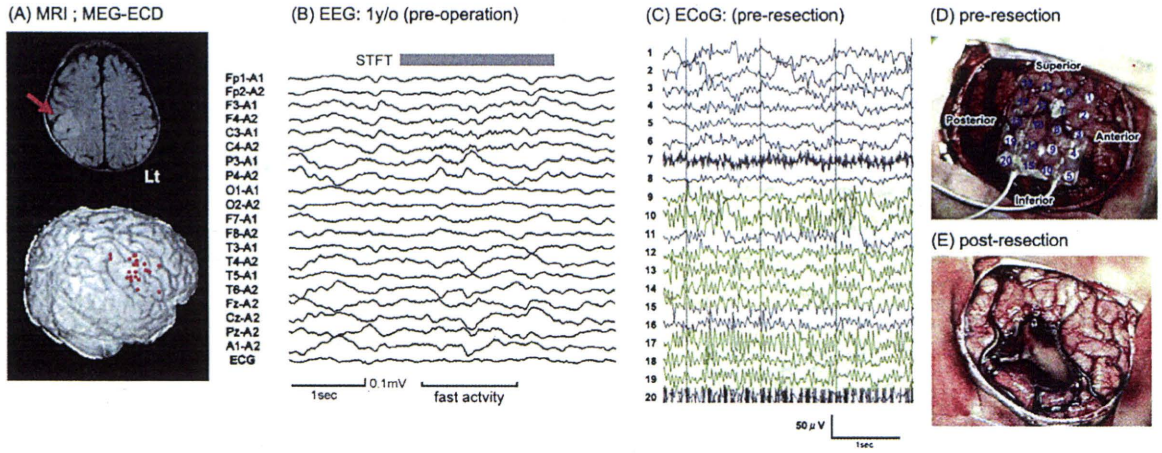

Figure 1 (A) Top panel: FLAIR MRI showing FCD on right parietal–occipital areas. Bottom panel: ECDs located at the FCD (red dot). (B) EEG at 1 year of age, just before the operation, demonstrating fast activity discharges at electrode C3, C4 interictally. (C) ECoG during operation before resection of lesion indicates 18–22-Hz polyspike bursts at electrodes 9, 10, 12–15, 17, 18, and 19 (yellow bar). These electrodes are located on top of the FCD. (D) FCD was exposed at the right supra-marginal gyrus during the operation. (E) FCD was resected after the operation. (For interpretation of the references to color in this figure legend, the reader is referred to the web version of the article.)

MRI

MRI was acquired with a 1.5 T high-resolution MRI scanner (Magnetom VISION; Siemens AG, Erlangen, Germany) for both diagnostic purposes and co-registration with the MEG data. Axial T1-weighted images (WI), T2WI, fluid-attenuated inversion recovery (FLAIR) images, and gadolinium-enhanced T1WI were obtained.

Single-photon emission computed tomography (SPECT)

^{99m}Tc L-ethyl cysteinate dimer (^{99m}Tc-ECD)-SPECT was performed interictally and ictally for Patient 2, and interictally for Patient 3. We used a ring-type SPECT scanner (Headtome-SET070; Shimadzu Corp., Kyoto, Japan). The ^{99m}Tc-ECD was injected intravenously at a dose of 111 MBq into Patient 2 and at 600 MBq into Patient 3.

Positron emission tomography (PET)

^{18}F-Fluorodeoxyglucose (FDG)-PET and ^{11}C-flumazenil (FMZ)-PET were performed for Patient 2 using the EXACT ECAT HR+ head scanner (Siemens). The injected doses of ^{18}F-FDG and ^{11}C-FMZ were 185 MBq and 370 MBq, respectively.

Results

Case reports

Patient 1

A 17-month-old boy had daily seizures. At 1 month of age, he began to have daily seizures with loss of consciousness and tonic extension of bilateral upper limbs. His seizure was refractory to various anti-epileptic drugs. Initially, his MRI finding was normal. At 16 months of age, a circumscribed lesion appeared on MRI with low intensity in the T1WI, high intensity in the T2WI, and FLAIR in right supra-marginal gyrus (Fig. 1A). An interictal EEG revealed rare spikes at electrodes C4 and P4 and low-voltage 10–12-Hz fast activity at electrodes C3 and C4 (Fig. 1B).

The 204ch MEG corresponding to the EEG fast activity showed rhythmic activities in the right central temporal areas (Fig. 2A). The ECDs were scattered over the cortical lesion (Fig. 1A, bottom panel). STFT analysis indicated a specific aberrant 15–18-Hz oscillation in the right central temporal areas (Fig. 2C). The specific oscillation at 15–18 Hz was generated at the focal cortical dysplasia (FCD) in the moving image (Fig. 3A).

The patient underwent craniotomy at 18 months of age. Intraoperative ECoG showed 18–19-Hz polyspike bursts at electrodes 9, 10, 12–15, 17, 18, and 19. These electrodes were located upon the resected cortical lesion (Fig. 1C, yellow bar). The frequencies of the MEG rhythmic activities (15–18 Hz) and ECoG polyspike (18–22 Hz) were comparable, and the locations of the MEG and ECoG oscillation almost overlapped. A total lesionectomy was performed.

The pathology was focal cortical dysplasia with balloon cells (Palmini type 2B). The patient has remained seizure-free for 22 months and has developed steadily.

Patient 2

A 2-year-old girl had daily seizures. At age 10 months, she experienced an afebrile, generalized, tonic-clinic seizure. MRI showed a left frontal cortical construction anomaly. At 15 months of age, she began to have seizures with extension of her right arm and leg, flexion of her left arm and leg, and deviation of her head and eyes to the right. Although anti-epileptic drugs controlled the seizures, she was able to speak only a few words at 32 months of age.

T2WI and FLAIR MRI showed cortical thickening in the left frontal lobe, blurring of the gray-white matter junction and hyperintensity of the subcortical white matter. Interictal ^{99m}Tc-ECD-SPECT showed hypoperfusion in the left frontal area and ictal ^{99m}Tc-ECD-SPECT revealed hyperperfusion in the left frontal area. ^{18}F-FDG-PET showed hypometabolism in the left frontal area, and ^{11}C-FMZ PET demonstrated decreased binding at the left frontal area.

Interictal EEG demonstrated rhythmic, 13–14-Hz, low-voltage fast activity and a low number of sharp waves

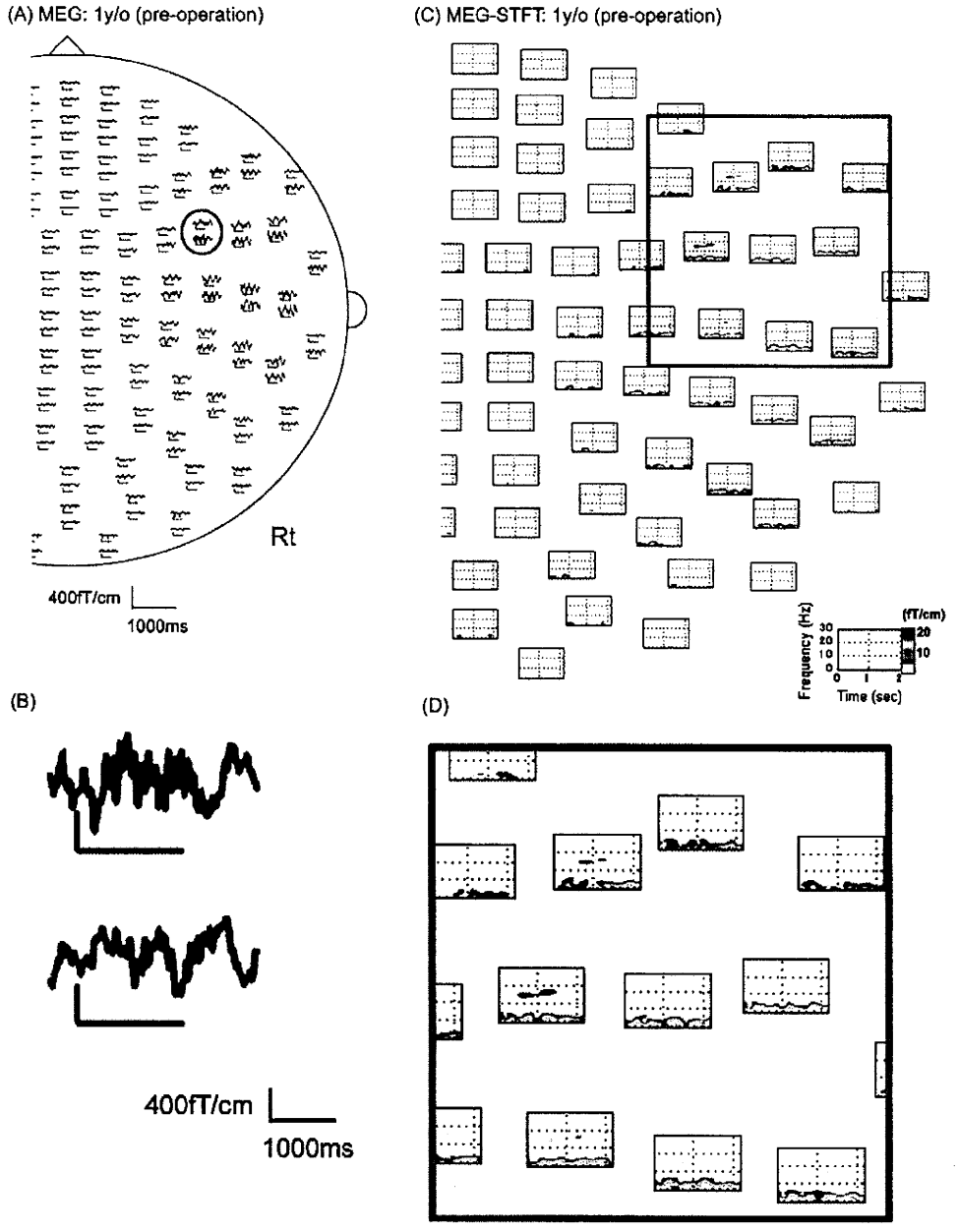

Figure 2 (A) 204ch MEG corresponding to interictal fast activity on the EEG (gray bar in Fig. 1B) demonstrates polyspikes at the right central temporal areas. (B) One representative gradiometer (red circle in (A)) showing rhythmic activity. (C) STFT graph showing specific rhythmic activities with 15–18-Hz oscillation at the right central temporal areas (red squire). (D) Enlarged section of red squire in (C). (For interpretation of the references to color in this figure legend, the reader is referred to the web version of the article.)

at electrodes Fp1, Fp2, F3, and F7. Ictal EEG showed desynchronization, followed by left frontal spikes and slow waves.

The 204ch MEG corresponding to the EEG fast activity showed rhythmic activities at the left frontal–temporal areas. The ECDs were not clustered due to the low number of isolated spikes with sufficient signal-to-noise ratio. STFT analysis indicated that a specific, aberrant, 15–20-Hz oscillation was generated at the left superior temporal gyrus and propagated to the middle and inferior frontal gyri in the moving image (Fig. 3B, top panel).

The patient underwent the operation at 36 months. Intraoperative ECoG showed 13–25-Hz spikes and polyspikes at the orbito-frontal area.

The frequencies of the MEG oscillation (15–20 Hz) and ECoG polyspike (13–25 Hz) were comparable. ECoG polyspikes were located inside the area where the MEG oscillation was depicted by moving images.